

---

# How Sampling Impacts the Robustness of Stochastic Neural Networks

---

**Sina Däubener and Asja Fischer**  
Department of Computer Science  
Ruhr University Bochum, Germany  
{sina.daeubener, asja.fischer}@rub.de

## Abstract

Stochastic neural networks (SNNs) are random functions whose predictions are gained by averaging over multiple realizations. Consequently, a gradient-based adversarial example is calculated based on one set of samples and its classification on another set. In this paper, we derive a sufficient condition for such a stochastic prediction to be robust against a given sample-based attack. This allows us to identify the factors that lead to an increased robustness of SNNs and gives theoretical explanations for: (i) the well known observation, that increasing the amount of samples drawn for the estimation of adversarial examples increases the attack’s strength, (ii) why increasing the number of samples during an attack can not fully reduce the effect of stochasticity, (iii) why the sample size during inference does not influence the robustness, and (iv) why a higher gradient variance and a shorter expected value of the gradient relates to a higher robustness. Our theoretical findings give a unified view on the mechanisms underlying previously proposed approaches for increasing attack strengths or model robustness and are verified by an extensive empirical analysis.

## 1 Introduction

Since the discovery of adversarial examples [Biggio et al., 2013, Szegedy et al., 2014], a significant amount of research was dedicated to hinder attacks [e.g. Madry et al., 2018, Papernot et al., 2016, Zhang et al., 2019], to enhance attack strategies [e.g. Athalye et al., 2018, Akhtar and Mian, 2018, Carlini and Wagner, 2017b, Uesato et al., 2018] or to derive ways to certify model robustness [e.g. Cohen et al., 2019, Lécuyer et al., 2019]. Robustness guarantees often specify an  $\epsilon$ -ball around input points in which perturbations do not lead to a label change [Hein and Andriushchenko, 2017, Croce and Hein, 2020]. The maximal possible radius of such an  $\epsilon$ -ball corresponds to the distance of the input point to the nearest decision boundary, which on the other hand is equal to the length of the smallest perturbation vector that leads to a misclassification (c.f. figure 1a)). Such a robustness analysis assumes that the decision boundaries are fixed and that the attacker is able to estimate (at least approximately) this minimal perturbation vector, which is a reasonable assumption for deterministic networks but usually does not hold for stochastic neural networks (SNNs).

Stochastic neural networks, and stochastic classifiers more generally, are random functions and predictions are given by the expected value of the random function for the given input. In practice, this expectation is usually not tractable and hence it is approximated by averaging over multiple realizations of the random function. This approximation leads to the challenging setting where predictions, decision boundaries, and gradients become random variables themselves. Hence, under an adversarial attack, the decision boundaries used for calculating the adversarial example and those used when predicting the label of the resulting adversarial example differ. This means that the attacker can not estimate the optimal perturbation direction i.e., the direction to the closest decision boundary of the network that will be sampled during inference c.f. figure 1 b), c).

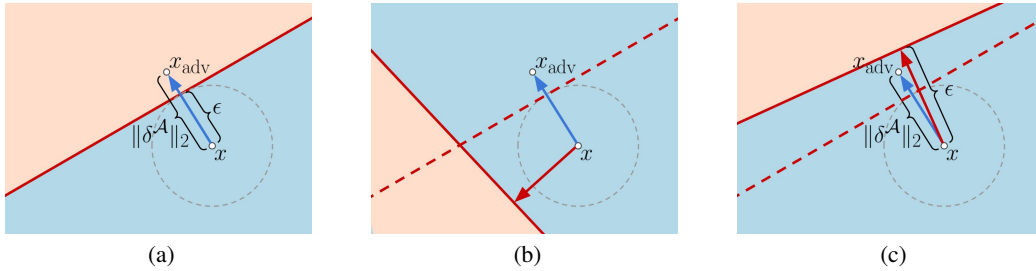


Figure 1: (Un-)successful attacks on a binary stochastic classifier with a linear decision boundary. a) an adversarial example  $x_{\text{adv}} = x + \delta^{\mathcal{A}}$  is created by shifting  $x$  in the direction of the closest decision boundary, indicated by the blue arrow.  $\epsilon$  is the minimal needed attack length and the attack can only be an adversarial example if  $\|\delta^{\mathcal{A}}\|_2 \geq \epsilon$  holds. b) and c) show the stochastic decision boundaries during attack (dashed) and inference (solid). The red arrows indicate the shortest direction to the latter, respectively. In b)  $\delta^{\mathcal{A}}$  moves  $x$  even further away from the decision boundary used during inference, while in c) the magnitude of  $\delta^{\mathcal{A}}$  is too short to result in a successful attack.

In this paper, we study how robustness of SNNs arises from this misalignment of the attack direction and the optimal perturbation direction during inference that results from the stochasticity inherent to stochastic classifiers.

We make the following contributions: First, we derive a sufficient condition for a SNN prediction relying on one set of samples to be robust against an attack that was calculated on a second set of samples. Second, we discuss how model properties and sample sizes impact this condition which does not only allows us to answer the questions stated in the abstract but also to explain the success of recently proposed defense mechanism from a simple unifying geometric perspective. Lastly, we conduct an empirical analysis that demonstrates that the novel theoretical insights perfectly match what we observe in practice.

## 2 Related work

Several works proposed stochastic defense mechanism to increase adversarial robustness [e.g. Raff et al., 2019, Xie et al., 2018]. Athalye et al. [2018] linked their success to gradient obfuscating during the attack and showed that increasing the number of samples for approximating the gradient during attack leads to a sever decrease in adversarial accuracy.

However, SNNs were still found to have an increased robustness even w.r.t. stronger attacks [Yu et al., 2021, He et al., 2019, Eustratiadis et al., 2021, Jeddi et al., 2020]. Their success was attributed to different effects of stochasticity, e.g. model smoothing [Liu et al., 2018, Addepalli et al., 2021] or diversification of the gradients [Lee et al., 2022, Bender et al., 2020]. While a lot of work analyzed the robustness of deterministic neural networks [e.g. Madry et al., 2018, Croce et al., 2019, Croce and Hein, 2020, Dabouei et al., 2020, Yang et al., 2022], the robustness of SNNs is less well understood. One line of research focused on the robustness of Bayesian neural networks (BNNs). Wicker et al. [2020] certified robustness of BNNs using interval bound propagation techniques which they later also employed to derive guarantees for the robustness of BNNs with modified adversarial training [Wicker et al., 2021]. Moreover, Carbone et al. [2020] investigate robustness in the infinite-width infinite-sample limit. Lastly, Pinot et al. [2019] derived theoretical robustness guarantees for randomized networks, where the randomization is based on additive noise from an exponential family distribution. This leads to a generalization of the robustness guarantees derived previously by Lécuyer et al. [2019] and Cohen et al. [2019]. Those certified robustness guarantees specify the radius of an  $\ell_2$ -ball in which the prediction does not change. In contrast, our results specify the robustness that results from the difficulty to identify the ideal attack direction and imply that even for perturbations outside this confidence ball, a gradient-based attack has a chance of not being successful.

To the best of our knowledge, no existing theoretical analysis of SNNs explicitly discusses either the effect of stochasticity during inference nor the impact of the sample size during attack and prediction on the robustness.

### 3 Preliminaries

We first clarify the terminology before we state the main theoretical results of our paper.

**Stochastic classifiers** We use the term *stochastic classifiers* for all classifiers which have an inherent stochasticity through the use of random variables in the model. Formally, we define them as follows:

**Definition 3.1** (Stochastic classifiers). A stochastic classifier with  $k$  classes corresponds to a function  $f : \mathbb{R}^d \times \Omega^h \rightarrow \mathbb{R}^k$  that maps a pair  $(x, \Theta)$  to the output  $f(x, \Theta) = (f_1(x, \Theta), \dots, f_k(x, \Theta))^T$ , where  $x \in \mathbb{R}^d$  is an input vector,  $\Theta \in \Omega^h$ ,  $\Theta \sim p(\Theta)$  is a random vector, and  $f_c(x, \Theta)$  with  $c \in \{1, \dots, k\}$  are the discriminant functions for each class. The prediction of a stochastic classifier for an input  $x$  is given by  $\mathbb{E}_\Theta[f(x, \Theta)]$  and the predicted class by  $\arg \max_c \mathbb{E}_\Theta[f_c(x, \Theta)]$ .

This generic definition of stochastic classifiers covers linear models with random weights, but also more complicated methods like BNNs [Neal, 1996], infinite mixtures [Däubener and Fischer, 2020], Monte Carlo dropout networks [Gal and Ghahramani, 2016], randomized smoothing as proposed by Lécuyer et al. [2019]<sup>1</sup>, and any other class of neural networks which use stochasticity at the input level [e.g. Raff et al., 2019] or within the network [e.g. He et al., 2019, Jeddi et al., 2020, Liu et al., 2018, Yu et al., 2021, Eustratiadis et al., 2021]. In cases where  $\mathbb{E}_\Theta[f(x, \Theta)]$  is not tractable — which is in practice usually the case — the prediction of the stochastic classifier is approximated by its Monte Carlo (MC) estimate  $f^S(x) := \frac{1}{S} \sum_{s=1}^S f(x, \theta_s)$ , where the samples in the sample set  $\mathcal{S} = \{\theta_1, \dots, \theta_S\}$  are drawn from  $p(\Theta)$ .

**Adversarial attacks on stochastic classifiers** Informally speaking, adversarial examples are inputs that are modified such that the network predicts wrong classes even though the changes to the inputs are not perceptible for a human. More precisely, let  $x$  be an input with corresponding true label  $y \in \{1, \dots, k\}$  that is classified correctly by the multi-class classifier  $f(\cdot)$ , that is  $\arg \max_c f_c(x) = y$ . We consider the most common attack form which aims at misclassifying  $x$  by allowing for some predefined maximum magnitude of perturbation. That is, the attacker targets the optimization problem

$$\text{maximize } \mathcal{L}(f(x + \delta), y) \quad , \quad \text{s.t. } \|\delta\|_p \leq \eta \quad , \quad (1)$$

where  $\mathcal{L}(\cdot, \cdot)$  is the loss function,  $\|\cdot\|_p$  with  $p \geq 1$  is the  $\ell_p$ -norm, and  $\eta$  is the *perturbation strength*, i.e. the maximal allowed magnitude of the attack (see figure 1a) for an illustration). Common choices of loss functions include the cross-entropy loss and the negative margin loss  $\mathcal{L}_{\text{margin}}(f(x + \delta), y) = -(f_y(x + \delta) - \max_{c \neq y} f_c(x + \delta))$ . In practice, targeting the optimization problem in eq. (1) usually involves estimating  $\delta$  by performing some kind of gradient-based optimization on the loss function [e.g. Goodfellow et al., 2015, Madry et al., 2018]. If  $f^S(\cdot)$  is a stochastic classifier (as introduced in the previous paragraph) approximated by its MC estimate, the loss gradient with respect to the input is stochastic as well and given by

$$\nabla_x \mathcal{L}(f^S(x), y) = \nabla_x \mathcal{L} \left( \frac{1}{S} \sum_{s=1}^S f(x, \theta_s), y \right) \quad . \quad (2)$$

Note, that for linear  $\mathcal{L}$ , as for example the margin loss for a fixed class  $c$ , the loss gradient of the mean prediction is equivalent to the mean of the loss gradients for single sample predictions. However, in general (e.g. for the cross entropy loss) this is not the case.

### 4 Geometrical robustness analysis

After clarifying our understanding of stochastic classifiers and on how gradient-based adversarial attacks are conducted on them, we are now able to present a simple but general geometrical, adversarial robustness analysis for stochastic classifiers. It is motivated by the following observation: Each time a stochastic classifier is used for a prediction, another set of realizations from the random vectors are

<sup>1</sup>Note, that, in contrast to Lécuyer et al. [2019] the variant of randomized smoothing proposed by Cohen et al. [2019] does not define the prediction of the SNN to be given by the expectation over  $\Theta$  but by  $\arg \max_{c \in \mathcal{Y}} P(f(x + \epsilon) = c)$ , where  $\epsilon \sim \mathcal{N}(0, \sigma^2 I)$ . This makes our results not directly applicable to their networks. However, they can probably be transferred to the decision boundaries and attacks corresponding to their form of generating predictions.

drawn, resulting in another set of discriminant functions and corresponding decision boundaries. To put it into other words, the classifier gets a random variable itself. As a consequence, calculating a gradient-based adversarial attack for an input  $x$  is done with respect to a drawn set of realizations  $\mathcal{A} = \{\theta_1^a, \theta_2^a, \dots, \theta_{S^{\mathcal{A}}}^a\}$ , and thus  $\delta$  from eq. (1) is specific for a realization  $f^{\mathcal{A}}(x)$  of the classifier, which we specify by writing  $\delta^{\mathcal{A}}$ . During inference, the resulting adversarial example  $x_{\text{adv}} = x + \delta^{\mathcal{A}}$  is then fed to another random classifier  $f^{\mathcal{I}}$ , which is based on a different set of realizations from the random vector  $\mathcal{I} = \{\theta_1^i, \theta_2^i, \dots, \theta_{S^{\mathcal{I}}}^i\}$ . From this perspective, the prediction model  $f^{\mathcal{I}}$  is robust against the attack if the distance from  $x$  to the decision boundary (given by  $f_y^{\mathcal{I}}(x) - f_{c \neq y}^{\mathcal{I}}(x) = 0$ ) in the *direction* of  $\delta^{\mathcal{A}}$  is larger than the length of  $\delta^{\mathcal{A}}$ , as illustrated in figures 1b) and c).

**Robustness conditions for stochastic attacks** For a classifier with linear discriminant functions, we are able to turn the previously described observation into a theorem in which we derive a sufficient and necessary condition for the prediction model to be robust against a given attack.

**Theorem 4.1** (Sufficient and necessary robustness condition for linear classifiers). *Let  $f : \mathbb{R}^d \times \Omega^h \rightarrow \mathbb{R}^k$  be a stochastic classifier with linear discriminant functions and  $f^{\mathcal{A}}$  and  $f^{\mathcal{I}}$  be two MC estimates of the classifier. Let  $x \in \mathbb{R}^d$  be a data point with label  $y \in \{1, \dots, k\}$  and  $\arg \max_c f_c^{\mathcal{A}}(x) = \arg \max_c f_c^{\mathcal{I}}(x) = y$ , and let  $x_{\text{adv}} = x + \delta^{\mathcal{A}}$  be an adversarial example computed for solving the minimization problem (1) for  $f^{\mathcal{A}}$ . It holds that  $\arg \max_c f_c^{\mathcal{I}}(x + \delta^{\mathcal{A}}) = y$  if and only if*

$$\min_{c \neq y} \tilde{r}_c^{\mathcal{I}} > \|\delta^{\mathcal{A}}\|_2, \text{ with} \quad (3)$$

$$\tilde{r}_c^{\mathcal{I}} = \begin{cases} \infty, & \text{if } \cos(\alpha_c^{\mathcal{I}, \mathcal{A}}) = \frac{\langle -\nabla_x(f_y^{\mathcal{I}}(x) - f_c^{\mathcal{I}}(x)), \delta^{\mathcal{A}} \rangle}{\|\nabla_x(f_y^{\mathcal{I}}(x) - f_c^{\mathcal{I}}(x))\|_2 \cdot \|\delta^{\mathcal{A}}\|_2} \leq 0 \\ \frac{f_y^{\mathcal{I}}(x) - f_c^{\mathcal{I}}(x)}{\|\nabla_x(f_y^{\mathcal{I}}(x) - f_c^{\mathcal{I}}(x))\|_2 \cdot \cos(\alpha_c^{\mathcal{I}, \mathcal{A}})}, & \text{otherwise,} \end{cases}$$

where  $\alpha_c^{\mathcal{I}, \mathcal{A}}$  is the angle between  $-\nabla_x(f_y^{\mathcal{I}}(x) - f_c^{\mathcal{I}}(x))$  and  $\delta^{\mathcal{A}}$ .

The proof which is based on Taylor expansion is given in supplement A. The conditions for  $\cos(\alpha_c^{\mathcal{I}, \mathcal{A}})$  have a nice geometrical interpretation: An angle of more than  $90^\circ$  (which corresponds to a negative cosine value) indicates that the gradient  $-\nabla_x(f_y^{\mathcal{I}}(x) - f_c^{\mathcal{I}}(x))$  and the perturbation  $\delta^{\mathcal{A}}$  point into “opposite” directions and thus even for infinitely long moves into the direction of  $\delta^{\mathcal{A}}$ , the predicted label for  $x$  will not change to class  $c \neq y$ . For positive cosine values,  $\tilde{r}_c^{\mathcal{I}}$  specifies the distance to the decision boundary in the attack direction. It looks similar to the minimal distance to the decision boundary in a deterministic setting which is given by  $\frac{f_y(x) - f_c(x)}{\|\nabla_x(f_y(x) - f_c(x))\|_2}$  and which is recovered if  $\cos(\alpha_c^{\mathcal{I}, \mathcal{A}}) = 1$ . A cosine value of one however can only occur if the gradient and perturbation direction are identical i.e., if the margin loss is used for calculating the attack direction and if attack and inference model are identical. In practice, the latter is almost surely not the case due to the finite sample approximation, and thus  $\cos(\alpha_c^{\mathcal{I}, \mathcal{A}}) < 1$ . This illustrates the robustness advantage induces by stochasticity.

The derived conditions may locally hold for classifiers which can be reasonably well approximated by a first-order Taylor approximation. To derive further guarantees, we can relax the linearity assumption by assuming discriminant functions which are  $L$ -smooth as defined in the following.

**Definition 4.1** ( $L$ -smoothness [Yang et al., 2022]). A differentiable function  $f : \mathbb{R}^d \rightarrow \mathbb{R}^k$  is  $L$ -smooth, if for any  $x_1, x_2 \in \mathbb{R}^d$  and any output  $c \in \{1, \dots, k\}$ :

$$\frac{\|\nabla_{x_1} f_c(x_1) - \nabla_{x_2} f_c(x_2)\|_2}{\|x_1 - x_2\|_2} \leq L.$$

For such smooth discriminant function we can derive a sufficient (but not necessary<sup>2</sup>) robustness condition specified by the following theorem, which is proven in supplement A.

**Theorem 4.2** (Sufficient condition for the robustness of a  $L$ -smooth stochastic classifier). *In the setting of Theorem 4.1, let  $f^{\mathcal{A}}$  and  $f^{\mathcal{I}}$  be  $L$ -smooth (instead of linear) discriminant functions. Then it*

<sup>2</sup>The necessity of this condition is not given since for non-linear decision boundaries it is possible that behind a region of a different class there exists another region of class  $y$  that an attack ends in if  $\delta^{\mathcal{A}}$  is long enough.

holds that  $\arg \max_c f_c^{\mathcal{I}}(x + \delta^{\mathcal{A}}) = y$  if  $\min_{c \neq y} r_c^{\mathcal{I}} > \|\delta^{\mathcal{A}}\|_2$  with

$$r_c^{\mathcal{I}} = \begin{cases} \infty, & \text{if } \|\nabla_x(f_y^{\mathcal{I}}(x) - f_c^{\mathcal{I}}(x))\|_2 \cdot \cos(\alpha_c^{\mathcal{I}, \mathcal{A}}) + \frac{L}{2} \cdot \|\delta^{\mathcal{A}}\|_2 \leq 0, \\ \frac{f_y^{\mathcal{I}}(x) - f_c^{\mathcal{I}}(x)}{\|\nabla_x(f_y^{\mathcal{I}}(x) - f_c^{\mathcal{I}}(x))\|_2 \cdot \cos(\alpha_c^{\mathcal{I}, \mathcal{A}}) + \frac{L}{2} \cdot \|\delta^{\mathcal{A}}\|_2}, & \text{otherwise} \end{cases}$$

with  $\cos(\alpha_c^{\mathcal{I}, \mathcal{A}})$  as in theorem 4.1.

**Factors influencing the robustness of stochastic classifiers** Since in practice neither the parameter set  $\mathcal{A}$  nor  $\mathcal{I}$  is fixed, the quantity better describing the practical robustness of a stochastic classifier with linear discriminant functions is

$$\mathbb{P}(\min_{c \neq y} \tilde{r}_c^{\mathcal{I}} > \|\delta^{\mathcal{A}}\|_2), \quad (4)$$

where  $\tilde{r}_c^{\mathcal{I}}$  and  $\delta^{\mathcal{A}}$  are random variables. For  $L$ -smooth models, replacing  $\tilde{r}_c^{\mathcal{I}}$  by  $r_c^{\mathcal{I}}$  leads to a lower bound on the robustness. Deriving an analytic expression for this probability is a hard problem. However, based on theorems 4.1 and 4.2 it becomes clear that a larger  $\min_{c \neq y} \tilde{r}_c^{\mathcal{I}}$  relates to increasing the probability in eq. (4) and thus to an increased robustness. We note that  $\tilde{r}_c^{\mathcal{I}}$  with  $c \neq y$  grows with i) larger prediction margins  $f_y^{\mathcal{I}}(x) - f_c^{\mathcal{I}}(x)$ , ii) smaller gradient norms  $\|\nabla_x(f_y^{\mathcal{I}}(x) - f_c^{\mathcal{I}}(x))\|_2$ , and iii) larger angles  $\alpha_c^{\mathcal{I}, \mathcal{A}}$ . Larger prediction margins and smaller gradient norms were also found to positively impact the robustness of deterministic networks [e.g. Ross and Doshi-Velez, 2018]. In contrast, the dependency on the angle is unique to the stochastic setting. We therefore focus on the analysis of this factor in the following.

**Analyzing the expected angle** The angle  $\alpha_c^{\mathcal{I}, \mathcal{A}}$  depends on both terms  $-\nabla_x(f_y^{\mathcal{I}}(x) - f_c^{\mathcal{I}}(x))$  (for which we use the shorthand  $-\nabla_x f_{y-c}^{\mathcal{I}}(x)$  in the following) and  $\delta^{\mathcal{A}}$ . For further analysis, we first rewrite the gradient as

$$-\nabla_x f_{y-c}^{\mathcal{I}}(x) = \nabla_x \left( \frac{1}{S^{\mathcal{I}}} \sum_{s=1}^{S^{\mathcal{I}}} -f_{y-c}(x, \theta_s^i) \right) = \frac{1}{S^{\mathcal{I}}} \sum_{s=1}^{S^{\mathcal{I}}} -\nabla_x f_{y-c}(x, \theta_s^i).$$

Let  $\mu = \mathbb{E}_{\Theta}[-\nabla_x f_{y-c}(x, \theta_s^i)]$  and  $\Sigma$  be the covariance of  $-\nabla_x f_{y-c}(x, \theta_s^i)$ , then it follows from the central limit theorem that for sufficiently many samples  $-\nabla_x f_{y-c}^{\mathcal{I}}(x) \sim \mathcal{N}(\mu, \frac{\Sigma}{S^{\mathcal{I}}})$ . For simplicity let us assume that the attack is based on the margin loss and only one iteration of gradient ascent. In this case,  $\delta^{\mathcal{A}} = \frac{\eta}{\|\hat{\delta}\|_2} \cdot \hat{\delta}$ , with  $\hat{\delta} \sim \mathcal{N}(\mu, \frac{\Sigma}{S^{\mathcal{A}}})$ . Note, that we can neglect the scaling of the attack vector, since the angle only depends on  $\hat{\delta}$ . Therefore, estimating the distribution of  $\alpha_c^{\mathcal{I}, \mathcal{A}}$  corresponds to estimating the distribution of the angle between two independent multivariate Gaussian random vectors with the same mean and (potentially) differently scaled versions of the same covariance.<sup>3</sup> It is known for vectors from normalized standard multivariate Gaussian distributions that the mode of the distribution of the angle between two random vectors is equal to 90° and that with increased dimension the concentration around this mode gets tighter [Cai et al., 2013]. Unfortunately, deriving a closed form expression for the distribution or expectation in the general case is a challenging task and beyond the scope of this paper. However, we conjecture that the expectation of the angle increases proportionally with the variance and anti-proportionally with the norm of the mean. We illustrate the intuition behind this hypothesis in figure 2. To empirically verify the correctness of this hypothesis we conducted an experiment where we estimated the expected angle between two identically distributed 1,000-dimensional Gaussian random vectors for different choices of means and diagonal covariances. More precisely, we sampled the mean and variances uniformly from  $[0, t]$ , where  $t$  increased from zero to ten with step size 0.2, and estimated the expected angle based on 10,000 vector pairs drawn from the resulting distributions. Results are shown in figure 2 on the right side. As hypothesized, the smaller the length of  $\mu$  and the higher the average variances, the higher the expected angle.

<sup>3</sup>In the case of more complicated attacks the mean will differ as well but we expect the findings of these section to generalize also to this scenario.

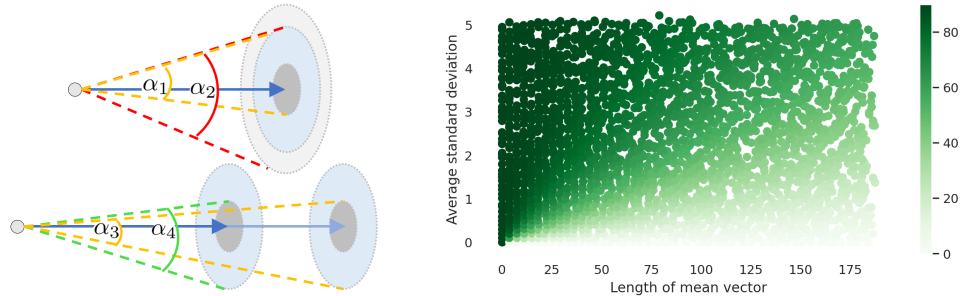


Figure 2: Dependence of the angle w.r.t mean and variance of the gradient. **Left, top:** Sketch of decreased variance which leads to smaller angles. The mean of the gradient is shown as the blue arrow. The circles indicate the areas of high probability for different scales of the covariance matrix. When the covariance is decreased (dark compared to light gray region) the maximum angle between vectors in these region to vectors from the blue region is decreased as well ( $\alpha_1$  compared to  $\alpha_2$ ). **Left, bottom:** Sketch of increased mean which leads to smaller maximal angles. When the covariance is fixed and the mean is increased (dark compared to light blue arrow) the maximum angle between vectors from high probability regions decreases ( $\alpha_3$  compared to  $\alpha_4$ ). **Right:** Expected angle between two identically distributed 1,000-dimensional Gaussian random vectors, for Gaussian with different means and variances. Expected angles were calculated based on 10,000 pairwise draws from the respective Gaussian distributions.

**Implications for the attack** Based on the previous discussion, the only way the attacker can influence the probability of a successful attack, and in this sense the robustness of the model against the attack, is by increasing the amount of samples and thereby reducing the variance of the attack vector. A reduction of the variance leads to a decrease of the expected angle as described in the previous section. This gives a more elaborated explanation of what was often loosely described as finding the “correct” gradient direction in previous work [Athalye et al., 2018]. However, even if the attacker would be able to take infinitely many samples, and thus the variance of the attack direction would be reduced to zero, the expected value of the angle will be larger than zero because of the still existing stochasticity in the inference process. This stochasticity can even lead to an expected angle close to  $90^\circ$  if  $\mu$  is short, and/or the covariance  $\Sigma$  is high. That is, the advantage of obfuscating the optimal attack direction by incorporating stochasticity into the classifier can be decreased but not fully counterbalanced by taking more samples during the attack. This might explain the finding in He et al. [2019], that the accuracy under attack stagnates at a higher level than the deterministic counterpart when increasing the number of iterations of iterative gradient-based attack methods.

**Implications for the model** From the perspective of the defender, the analysis of the angle shows that models with an increased gradient variance (which is often associated to a high prediction variance) and a small norm of the mean gradient are connected to larger values of  $\alpha_c^{\mathcal{I}, \mathcal{A}}$  and thus to a higher probability of unsuccessfully attacks. This explains why including the norm of the mean gradient, the gradient variance, or the angle between gradients as regularization terms in the training of SNNs, as for example proposed by Bender et al. [2020] and Lee et al. [2022]<sup>4</sup>, lead to an increased empirical robustness.

It would be naturally to suspect that increasing the number of samples used during inference also decreases the robustness, since it decreases the expected angle. However, this is not the case, as it is counterbalanced by an decrease of the norm of the gradient estimate (i.e. the second term in the denominator of  $\tilde{r}_c$ ) with growing sample size.<sup>5</sup> This can be seen by rewriting the expected denominator with respect to the two sample sets  $\mathcal{I}$  and  $\mathcal{A}$  as

<sup>4</sup>In these works the regularization terms were motivated by maintaining input sensitivity and bounding the expected loss increase, respectively.

<sup>5</sup>We present a proposition showing that the interval incorporating the gradient norm decreases to the norm of  $\mu$  with increasing amount of samples in supplement A.

$$\begin{aligned} \mathbb{E}_{\mathcal{I}, \mathcal{A}} [\|\nabla_x f_{y-c}^{\mathcal{I}}(x)\|_2 \cdot \cos(\alpha_c^{\mathcal{I}, \mathcal{A}})] &= \mathbb{E}_{\mathcal{I}, \mathcal{A}} \left[ \|\nabla_x f_{y-c}^{\mathcal{I}}(x)\|_2 \cdot \frac{\langle -\nabla_x f_{y-c}^{\mathcal{I}}(x), \delta^{\mathcal{A}} \rangle}{\|\nabla_x f_{y-c}^{\mathcal{I}}(x)\|_2 \cdot \|\delta^{\mathcal{A}}\|_2} \right] \\ &= \mathbb{E}_{\mathcal{I}, \mathcal{A}} \left[ \left\langle -\nabla_x f_{y-c}^{\mathcal{I}}(x), \frac{\delta^{\mathcal{A}}}{\|\delta^{\mathcal{A}}\|_2} \right\rangle \right] = \sum_{i=1}^p \mathbb{E}_{\mathcal{I}} [-\nabla_{x_i} f_{y-c}^{\mathcal{I}}(x)] \cdot \mathbb{E}_{\mathcal{A}} \left[ \frac{\delta_i^{\mathcal{A}}}{\|\delta^{\mathcal{A}}\|_2} \right], \end{aligned}$$

where the last equation holds due to the independence of  $\delta^{\mathcal{A}}$  and  $-\nabla_x f_{y-c}^{\mathcal{I}}(x)$ . The expectation of  $\frac{\delta_i^{\mathcal{A}}}{\|\delta^{\mathcal{A}}\|_2}$  does not depend on the samples taken during inference and the expectation of the estimate of the derivative w.r.t. the  $i$ -th input  $\mathbb{E}_{\mathcal{I}} [-\nabla_{x_i} f_{y-c}^{\mathcal{I}}(x)]$  is the same for different amounts of samples. Therefore, the expectation of the denominator does not change when changing the sample size during inference. This observation explains why the robustness of a stochastic classifier does not depend on the amount of samples taken during inference and gives an justification for picking an arbitrary sample size that allows for a good trade-off between efficiency and reduction of the variance of the MC estimate used for prediction.

## 5 Experimental robustness analysis

In this section we empirically demonstrate that the findings of our theoretical analysis are transferable to SNNs and help to explain the mechanisms leveraging the experimentally observed robustness of previously proposed SNNs.

**Experimental setup** Our experiments are conducted on two different image datasets: FashionMNIST [Xiao et al., 2017] and CIFAR10 [Krizhevsky et al., a].<sup>6</sup> For experiments on FashionMNIST we used feedforward neural networks (FNN) with two stochastic hidden layers, each with 128 neurons. We trained the FNN as a Variational Matrix Gaussian (VMG, the BNN proposed by Louizos and Welling [2016]) via variational inference or as an infinite mixture (IM) with the maximum likelihood objective proposed by Däubener and Fischer [2020], with matrix variate normal distribution placed over the weights. We also trained FNNs of the same architecture, where we added Gaussian noise with  $\sigma^2 = \{0.05, 0.1\}$  to the input, by minimizing the cross-entropy. We refer to these models as *stochastic input networks* (SINs) 0.05 and SIN 0.1, respectively. Note, that these networks correspond to the basic networks proposed for randomized smoothing by Lécuyer et al. [2019]. For experiments on CIFAR10 we trained two wide residual networks (ResNet) with MC dropout layers [Gal and Ghahramani, 2016] applied after the convolution blocks and dropout probabilities  $p = 0.3$  and  $p = 0.6$ . If not specified otherwise we used 100 samples of  $p(\Theta)$  for inference on all datasets and calculated adversarial attacks with the fast gradient (sign) method (FGM) [Goodfellow et al., 2015], the cross-entropy loss for IMs, BNNs, and ResNets, the margin loss  $\mathcal{L}_{\text{margin}}$  specified in section 3 for SINs, and the  $\ell_2$ -norm constraint based on the CleverHans repository [Papernot et al., 2018]. All experiments were run on a single NVIDIA GeForce RTX 2080 Ti. We refer the reader to supplement B for more details on the datasets, models, and the training procedure.

**Accuracy of robustness conditions** We first investigated the practical transferability of the derived theorems. For enforcing the smoothness condition used in theorem 4.2, we built on the result from Yang et al. [2022], who showed that the  $L$ -smoothness parameter of a classifier  $g : x \rightarrow \mathbb{E}_{\epsilon}[f(x + \epsilon)]$  smoothed with random noise  $\epsilon \sim \mathcal{N}(0, \sigma^2)$ , is bounded by  $L \leq 2/\sigma^2$ . We therefore applied randomized smoothing during training of the models. For the BNN, on which

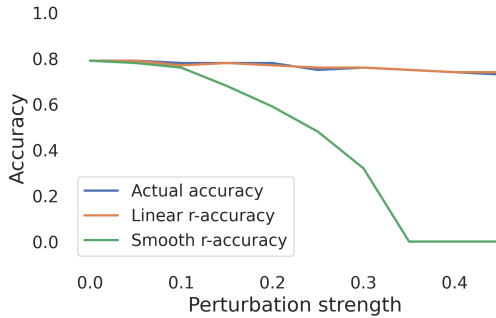


Figure 3: Adversarial accuracy of the smoothed BNN model for attacks based on 10 samples vs percentage of images with  $\min_c r_c^{\mathcal{I}} > \|\delta^{\mathcal{A}}\|_2$  (smooth) and  $\min_c \tilde{r}_c^{\mathcal{I}} > \|\delta^{\mathcal{A}}\|_2$  (linear) for the first 100 images from the FashionMNIST dataset.

<sup>6</sup>Additional experiments for CIFAR100 are presented in the supplement C.5.

we focus in this section due to space restrictions (results for the other networks look qualitatively similar and can be found in supplement C), we replaced each image in the batch by two noisy copies with Gaussian noise  $\epsilon \sim \mathcal{N}(0, 0.1)$  which ensures  $L \leq 20$ . During prediction we estimated the expectation under Gaussian noise with 10 samples and also used 10 samples for calculating the FGM attack. We estimated the percentage of resulting attacks for which  $\min_c r_c^{\mathcal{I}} > \|\delta^{\mathcal{A}}\|_2$  and  $\min_c \tilde{r}_c^{\mathcal{I}} > \|\delta^{\mathcal{A}}\|_2$  and compared this to the adversarial accuracy (i.e. the percentage of perturbed samples classified correctly) in figure 3. The percentage of samples fulfilling the condition  $\min_c r_c^{\mathcal{I}} > \|\delta^{\mathcal{A}}\|_2$  approaches zero with growing perturbation strength, indicating that the lower bound provided by  $r_c^{\mathcal{I}}$  is rather loose due to the high (upper bound of the) L-smoothness constant. On the other hand the percentage of samples for which (3) is fulfilled is a good approximation of the real accuracy for small attack length, which suggests that the discriminant functions are approximately linear in a small neighborhood of the input.

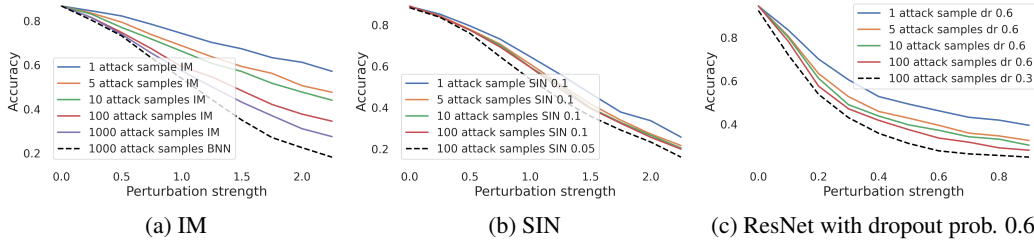


Figure 4: Accuracy under attack for different perturbation strength and amount of samples used for calculating the attack. The dashed line shows the adversarial accuracy for the models with the same architecture but less prediction variance.

**Stronger attacks by increased sample size** In this section we investigate the effect of varying the amount of samples used for calculating the attack, e.g. for  $S^{\mathcal{A}} \in \{1, 5, 10, 100, (1000)\}$ . Figure 4 shows the resulting adversarial robustness of the IM, SIN 0.1, and the ResNet with dropout probability 0.6. The accuracy under attack decreases for all models with increasing amount of samples used for calculating the attack as conjectured. We found this to hold also for stronger attacks, i.e. attacks based on logits for IM and BNN (where we observe highly confident softmax predictions), attacks with  $L_\infty$  constraint, or *projected gradient descent* (PGD) [Madry et al., 2018] attacks with 100 iterations as shown in supplement C. Note, that iterative attacks already increase the sample size due to their iterative nature, and therefore only few samples per iteration may sufficiently increase attack strength.

Simultaneously to the accuracy we estimated the corresponding values of  $\cos(\alpha_j^{\mathcal{I}, \mathcal{A}})$ , for  $j = \arg \min_c \tilde{r}_c^{\mathcal{I}}$ , for the first 1,000 test images and depicted them in figure 5. It can be seen that the cosine values are increasing (which corresponds to decreasing angles) with growing sample size and that the larger the observed values, the lower the accuracy under attack as shown in figure 4. This observation is in accordance to our theoretical analysis which predicts that an increased amount of samples leads to higher cosine values and in turn to less adversarial robustness. Note however, that even when taking many samples  $\cos(\alpha_j^{\mathcal{I}, \mathcal{A}}) < 1$ , which underlines the fact that the optimal attack direction can not be recovered due to the still existing stochasticity in the inference procedure. Further results on the angle under different amounts of samples during attack can be found in supplement C.2.

**Prediction variance as robustness indicator** In this section we compare the properties of SNNs that have the same network architecture and a similar training procedure but different prediction variances. That is, we compare the BNN against the IM, SIN 0.05 against SIN 0.1, and the two ResNets with different dropout probabilities against each other. First, we estimated the standard deviation of the prediction and the average standard deviation of the gradient entries of the models by calculating the average of the empirical estimates over the first 1,000 examples from the respective test sets (see table 1). As expected, the IM, SIN 0.1, and ResNet with dropout probability 0.6 have a larger standard deviation of the prediction and hence prediction variance than their respective counterpart. The higher standard deviation of the prediction translates to an increased standard deviation of the gradient. This explains why we observe smaller cosine values for these models compared to their counterparts (see right most boxplots in figure 5 a) and c)) which in turn translate

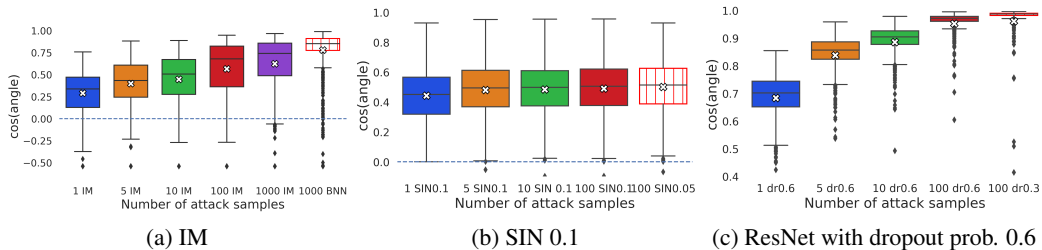


Figure 5: Cosine values for adversarial examples with perturbation strength 1.5 for a) and b) and 0.3 for c) and different amounts of samples. White crosses indicate mean values.

Table 1: Empirical standard deviation of the prediction (for the correct class) based on 1,000 single predictions (each with 1 inference sample) and average length and variance of the corresponding gradient. We report averages over the first 1,000 images from the respective test set.

	FASHIONMNIST				CIFAR10	
	BNN	IM	SIN 0.05	SIN 0.1	DR 0.3	DR 0.6
AVG. STD OF PREDICTIONS	0.0186	0.0473	85.4657	186.5599	0.0146	0.0196
AVG. GRADIENT LENGTH	0.5218	0.5044	49.0120	48.8312	0.0713	0.0599
AVG. STD OF GRADIENT	0.0316	0.0959	1.5741	1.8323	0.0000	0.0000

to an increased robustness (as indicated by the dotted accuracy curves in figure 4). We also found that the length of the mean of the gradient that we estimated based on 1,000 samples is smaller for the models with higher variance.<sup>7</sup> This might be another reason for the observed smaller angles as discussed in the previous section.

**Robustness in dependence of the amount of samples used during inference** In practice the amount of samples  $S^{\mathcal{I}}$  drawn during inference is fixed to an arbitrary number. In this section we investigate the impact of varying  $S^{\mathcal{I}} \in \{1, 5, 10, 100\}$  which are values frequently used. First, we observed that only few samples are necessary to get reliable predictions on clean data for all models as shown by the test accuracies in table 2. Second, we found that increasing the amount of samples did not affect the adversarial accuracy. This can be explained by the observation that the decrease of  $\alpha_c^{\mathcal{I}, \mathcal{A}}$  caused by increasing the sample set is counterbalanced by an simultaneous decrease of the average norm of the gradient estimate, as can be seen by inspecting the results in figure 6. That is, the product  $\|\nabla_x f_{y-c}^{\mathcal{I}}\|_2 \cdot \cos(\alpha_c^{\mathcal{I}, \mathcal{A}})$  stays approximately the same regardless of the inference sample size as predicted by our theoretical analysis. Interestingly, the effect of increasing the number of samples during inference has almost no effect on the prediction margin (more results are shown in supplement C.4).

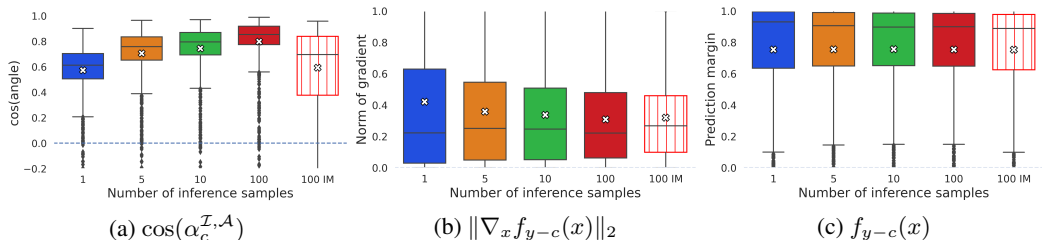


Figure 6: Values of single factors of  $\tilde{r}_c^{\mathcal{I}}$  in dependence of varying number of samples used during inference for the BNN trained on FashionMNIST.

<sup>7</sup>For SInS, it is known that a higher variance used during training relates to a lower Lipschitz-constant [e.g. Yang et al., 2022, Salman et al., 2019] which leads to a stronger smoothing effect.

Table 2: Test set and adversarial accuracy with 100 samples during the attack and allowed perturbation strength of 1.5 on FashionMNIST and 0.3 on CIFAR10 for increasing number of samples used during prediction. We estimated the average accuracy 10 times and report the average and standard deviation.

Z	FASHIONMNIST				CIFAR10	
	BNN	IM	SIN 0.05	SIN 0.1	DR 0.3	DR 0.6
TEST SET ACCURACY						
1	83.03 ± 0.12	79.15 ± 0.27	86.98 ± 0.17	85.76 ± 0.17	92.08 ± 0.13	92.68 ± 0.15
5	84.81 ± 0.14	84.29 ± 0.21	88.21 ± 0.09	87.49 ± 0.15	92.57 ± 0.05	93.51 ± 0.09
10	85.03 ± 0.13	85.02 ± 0.18	88.47 ± 0.06	87.92 ± 0.10	92.66 ± 0.06	93.60 ± 0.06
100	85.21 ± 0.06	85.72 ± 0.08	88.63 ± 0.07	88.27 ± 0.06	92.74 ± 0.03	93.69 ± 0.04
ADVERSARIAL ACCURACY						
1	35.76 ± 0.92	44.67 ± 1.19	36.15 ± 0.79	40.63 ± 0.79	42.64 ± 0.39	47.18 ± 0.70
5	36.19 ± 0.47	47.08 ± 0.73	35.92 ± 0.51	40.57 ± 0.44	42.73 ± 0.31	47.00 ± 0.38
10	36.30 ± 0.50	47.23 ± 0.62	36.06 ± 0.41	39.93 ± 0.66	42.69 ± 0.37	47.01 ± 0.33
100	36.50 ± 0.39	47.96 ± 0.24	35.91 ± 0.23	39.67 ± 0.29	42.82 ± 0.17	47.02 ± 0.20

## 6 Conclusion

In this work we have stressed the fact that stochastic neural networks (SNNs) (and stochastic classifiers in general) often depend on samples and thus their predictions are random variables themselves. For gradient-based adversarial attacks this means that the attack is calculated based on one realization of the stochastic network (which depends on multiple samples of the random variables used in the network) and applied to another which is used for inference. We derived a sufficient condition for this inference network to be robust against the calculated attack. This allowed us to identify the factors that lead to an increased robustness of stochastic classifiers: i) larger prediction margins ii) a smaller norm of the gradient estimates and iii) higher angles between the attack direction and the direction to the closest decision boundary during inference. The observed angles depend inverse proportionally on the norm of the expected gradient and proportionally on the variance of the gradient estimates. This variance can be reduced by increasing the sample size. These insights enable us to explain previously reported empirical findings for SNNs from a geometrical perspective, e.g. that the robustness of SNNs is higher than the robustness of their deterministic counterparts even for strong attacks that are based on several samples [He et al., 2019, Eustratiadis et al., 2021], why regularization of the gradient variance [Bender et al., 2020], norm of the mean gradient, and angle [Lee et al., 2022] improves the adversarial robustness, and last but not least why increasing the sample size during attack is important to exploit its potential [Athalye et al., 2018]. Therefore, our work poses a general applicable and simple framework, that helps understanding the mode of operation of existing stochastic defense mechanisms, even if they were motivated from a different point of view. Moreover, we derived a justification for the common practice of choosing the sample size during inference in a way that balances its prediction certainty against the computational cost. Finally, we believe our findings will be useful to evaluate and compare the robustness of different models, since they point out that they might require different amounts of samples during attack to sufficiently reduce variance and hope that they will help to improve the robustness of stochastic classifiers in future.

**Potential negative societal impact and limitations.** Since we do not propose a new attack strategy, but contribute to a better understanding of the robustness of SNNs and advise to cautiousness when determining sample sizes, we do not see negative impact.

## Acknowledgments

We would like to thank Denis Lukovnikov for his useful comments on our work and beautifying our graphics. This work is funded by the Deutsche Forschungsgemeinschaft (DFG, German Research Foundation) under Germany’s Excellence Strategy - EXC 2092 CASA - 390781972.

## References

- Sravanti Addepalli, Samyak Jain, Gaurang Sriramanan, and R. Venkatesh Babu. Boosting adversarial robustness using feature level stochastic smoothing. In *Proceedings of the IEEE/CVF Conference on Computer Vision and Pattern Recognition (CVPR) Workshops*, pages 93–102, 2021.
- Naveed Akhtar and Ajmal Mian. Threat of adversarial attacks on deep learning in computer vision: A survey. *IEEE Access*, 6:14410–14430, 2018.
- Anish Athalye, Nicholas Carlini, and David A. Wagner. Obfuscated gradients give a false sense of security: Circumventing defenses to adversarial examples. In *Proceedings of the 35th International Conference on Machine Learning (ICML)*, pages 274–283, 2018.
- Christopher Bender, Yang Li, Yifeng Shi, Michael K. Reiter, and Junier Oliva. Defense through diverse directions. In *Proceedings of the 37th International Conference on Machine Learning (ICML)*, pages 756–766, 2020.
- Battista Biggio, Iginio Corona, Davide Maiorca, Blaine Nelson, Nedim Šrndić, Pavel Laskov, Giorgio Giacinto, and Fabio Roli. Evasion attacks against machine learning at test time. In Hendrik Blockeel, Kristian Kersting, Siegfried Nijssen, and Filip Železný, editors, *Machine Learning and Knowledge Discovery in Databases*, pages 387–402. Springer Berlin Heidelberg, 2013.
- Sébastien Bubeck. Convex optimization: Algorithms and complexity. In *arXiv preprint <https://arxiv.org/pdf/1405.4980>*, 2015.
- Tony Cai, Jianqing Fan, and Tiefeng Jiang. Distributions of angles in random packing on spheres. *Journal of Machine Learning Research*, 14(21):1837–1864, 2013.
- Ginevra Carbone, Matthew Wicker, Luca Laurenti, Andrea Patane', Luca Bortolussi, and Guido Sanguinetti. Robustness of bayesian neural networks to gradient-based attacks. In *Advances in Neural Information Processing Systems (NeurIPS)*, volume 33, pages 15602–15613, 2020.
- Nicholas Carlini and David Wagner. Towards evaluating the robustness of neural networks. In *IEEE Symposium on Security and Privacy (SP)*, pages 39–57, 2017a.
- Nicholas Carlini and David Wagner. *Adversarial Examples Are Not Easily Detected: Bypassing Ten Detection Methods*, page 3–14. Association for Computing Machinery, 2017b.
- Jeremy Cohen, Elan Rosenfeld, and Zico Kolter. Certified adversarial robustness via randomized smoothing. In *Proceedings of the 36th International Conference on Machine Learning (ICML)*, volume 97, pages 1310–1320, 2019.
- Francesco Croce and Matthias Hein. Provable robustness against all adversarial  $l_p$ -perturbations for  $p \geq 1$ . In *International Conference on Learning Representations (ICLR)*, 2020.
- Francesco Croce, Maksym Andriushchenko, and Matthias Hein. Provable robustness of relu networks via maximization of linear regions. In *Proceedings of the Twenty-Second International Conference on Artificial Intelligence and Statistics (AISTATS)*, volume 89, pages 2057–2066, 2019.
- Ali Dabouei, Sobhan Soleymani, Fariborz Taherkhani, Jeremy Dawson, and Nasser M. Nasrabadi. Exploiting joint robustness to adversarial perturbations. In *IEEE/CVF Conference on Computer Vision and Pattern Recognition (CVPR)*, pages 1119–1128, 2020.
- Erik Daxberger, Agustinus Kristiadi, Alexander Immer, Runa Eschenhagen, Matthias Bauer, and Philipp Hennig. Laplace redux—effortless Bayesian deep learning. In *Advances in Neural Information Processing Systems (NeurIPS)*, 2021.
- Sina Däubener and Asja Fischer. Investigating maximum likelihood based training of infinite mixtures for uncertainty quantification. In *arXiv preprint <https://arxiv.org/abs/2008.03209>*, 2020.
- Panagiotis Eustratiadis, Henry Gouk, Da Li, and Timothy Hospedales. Weight-covariance alignment for adversarially robust neural networks. In *Proceedings of the 38th International Conference on Machine Learning (ICML)*, volume 139, pages 3047–3056, 2021.

- Yarin Gal and Zoubin Ghahramani. Dropout as a bayesian approximation: Representing model uncertainty in deep learning. In *Proceedings of The 33rd International Conference on Machine Learning (ICML)*, volume 48, pages 1050–1059, 2016.
- Ian J. Goodfellow, Jonathon Shlens, and Christian Szegedy. Explaining and harnessing adversarial examples. In *3rd International Conference on Learning Representations, (ICLR)*, 2015.
- Sven Gowal, Chongli Qin, Jonathan Uesato, Timothy Mann, and Pushmeet Kohli. Uncovering the limits of adversarial training against norm-bounded adversarial examples. *arXiv preprint*, 2020. URL <https://arxiv.org/pdf/2010.03593>.
- Zhezhi He, Adnan Siraj Rakin, and Deliang Fan. Parametric noise injection: Trainable randomness to improve deep neural network robustness against adversarial attack. In *Proceedings of the IEEE/CVF Conference on Computer Vision and Pattern Recognition (CVPR)*, 2019.
- Matthias Hein and Maksym Andriushchenko. Formal guarantees on the robustness of a classifier against adversarial manipulation. In *Advances in Neural Information Processing Systems (NeurIPS)*, volume 30, 2017.
- Ahmadreza Jeddi, Mohammad Javad Shafiee, Michelle Karg, Christian Scharfenberger, and Alexander Wong. Learn2perturb: An end-to-end feature perturbation learning to improve adversarial robustness. In *2020 IEEE/CVF Conference on Computer Vision and Pattern Recognition (CVPR)*, pages 1238–1247, 2020.
- Diederik P. Kingma and Jimmy Ba. Adam: A method for stochastic optimization. In *3rd International Conference on Learning Representations (ICLR)*, 2015.
- Alex Krizhevsky, Vinod Nair, and Geoffrey Hinton. Cifar-10 (canadian institute for advanced research). In <http://www.cs.toronto.edu/~kriz/cifar.html>, a.
- Alex Krizhevsky, Vinod Nair, and Geoffrey Hinton. Cifar-10, cifar-100 (canadian institute for advanced research). In <http://www.cs.toronto.edu/~kriz/cifar.html>, b.
- Mathias Lécuyer, Vaggelis Atlidakis, Roxana Geambasu, Daniel Hsu, and Suman Jana. Certified robustness to adversarial examples with differential privacy. In *IEEE Symposium on Security and Privacy (SP)*, pages 656–672, 2019.
- Sungyoon Lee, Hoki Kim, and Jaewook Lee. Graddiv: Adversarial robustness of randomized neural networks via gradient diversity regularization. *IEEE Transactions on Pattern Analysis and Machine Intelligence*, pages 1–1, 2022.
- Xuanqing Liu, Minhao Cheng, Huan Zhang, and Cho-Jui Hsieh. Towards robust neural networks via random self-ensemble. In *Computer Vision – ECCV*, pages 381–397, 2018.
- Christos Louizos and Max Welling. Structured and efficient variational deep learning with matrix gaussian posteriors. In *Proceedings of The 33rd International Conference on Machine Learning (ICML)*, volume 48, pages 1708–1716, 2016.
- David J. C. MacKay. A practical bayesian framework for backpropagation networks. *Neural Comput.*, 4(3):448–472, 1992. ISSN 0899-7667.
- Aleksander Madry, Aleksandar Makelov, Ludwig Schmidt, Dimitris Tsipras, and Adrian Vladu. Towards deep learning models resistant to adversarial attacks. In *International Conference on Learning Representations (ICLR)*, 2018.
- Radford M. Neal. *Bayesian Learning for Neural Networks*. Springer-Verlag, Berlin, Heidelberg, 1996.
- Nicolas Papernot, Patrick McDaniel, Xi Wu, Somesh Jha, and Ananthram Swami. Distillation as a defense to adversarial perturbations against deep neural networks. In *IEEE Symposium on Security and Privacy (SP)*, pages 582–597, 2016.

- Nicolas Papernot, Fartash Faghri, Nicholas Carlini, Ian Goodfellow, Reuben Feinman, Alexey Kurakin, Cihang Xie, Yash Sharma, Tom Brown, Aurko Roy, Alexander Matyasko, Vahid Behzadan, Karen Hambardzumyan, Zhishuai Zhang, Yi-Lin Juang, Zhi Li, Ryan Sheatsley, Abhibhav Garg, Jonathan Uesato, Willi Gierke, Yinpeng Dong, David Berthelot, Paul Hendricks, Jonas Rauber, and Rujun Long. Technical report on the cleverhans v2.1.0 adversarial examples library. In *arXiv preprint <https://arxiv.org/abs/1610.00768>*, 2018.
- Rafael Pinot, Laurent Meunier, Alexandre Araujo, Hisashi Kashima, Florian Yger, Cedric Gouy-Pailler, and Jamal Atif. Theoretical evidence for adversarial robustness through randomization. In *Advances in Neural Information Processing Systems (NeurIPS)*, volume 32, 2019.
- Edward Raff, Jared Sylvester, Steven Forsyth, and Mark McLean. Barrage of random transforms for adversarially robust defense. In *IEEE/CVF Conference on Computer Vision and Pattern Recognition (CVPR)*, pages 6521–6530, 2019.
- Andrew Ross and Finale Doshi-Velez. Improving the adversarial robustness and interpretability of deep neural networks by regularizing their input gradients. *Proceedings of the AAAI Conference on Artificial Intelligence*, 32(1), 2018.
- Hadi Salman, Jerry Li, Ilya Razenshteyn, Pengchuan Zhang, Huan Zhang, Sebastien Bubeck, and Greg Yang. Provably robust deep learning via adversarially trained smoothed classifiers. In *Advances in Neural Information Processing Systems (NeurIPS)*, volume 32, 2019.
- Christian Szegedy, Wojciech Zaremba, Ilya Sutskever, Joan Bruna, Dumitru Erhan, Ian J. Goodfellow, and Rob Fergus. Intriguing properties of neural networks. In *2nd International Conference on Learning Representations (ICLR)*, 2014.
- Jonathan Uesato, Brendan O’Donoghue, Pushmeet Kohli, and Aäron van den Oord. Adversarial risk and the dangers of evaluating against weak attacks. In *Proceedings of the 35th International Conference on Machine Learning (ICML)*, volume 80, pages 5032–5041, 2018.
- Matthew Wicker, Luca Laurenti, Andrea Patane, and Marta Kwiatkowska. Probabilistic safety for bayesian neural networks. In *Proceedings of the Thirty-Sixth Conference on Uncertainty in Artificial Intelligence (UAI)*, volume 124, pages 1198–1207, 2020.
- Matthew Wicker, Luca Laurenti, Andrea Patane, Zhuotong Chen, Zheng Zhang, and Marta Kwiatkowska. Bayesian inference with certifiable adversarial robustness. In *Proceedings of The 24th International Conference on Artificial Intelligence and Statistics (AISTATS)*, volume 130, pages 2431–2439, 2021.
- Han Xiao, Kashif Rasul, and Roland Vollgraf. Fashion-mnist: a novel image dataset for benchmarking machine learning algorithms. In *arXiv preprint <https://arxiv.org/abs/1708.07747>*, 2017.
- Cihang Xie, Jianyu Wang, Zhishuai Zhang, Zhou Ren, and Alan Yuille. Mitigating adversarial effects through randomization. In *International Conference on Learning Representations (ICLR)*, 2018.
- Zhuolin Yang, Linyi Li, Xiaojun Xu, Bhavya Kailkhura, Tao Xie, and Bo Li. On the certified robustness for ensemble models and beyond. In *International Conference on Learning Representations (ICLR)*, 2022.
- Tianyuan Yu, Yongxin Yang, Da Li, Timothy Hospedales, and Tao Xiang. Simple and effective stochastic neural networks. *Proceedings of the AAAI Conference on Artificial Intelligence*, 35(4): 3252–3260, 2021.
- Sergey Zagoruyko and Nikos Komodakis. Wide residual networks. In *arXiv preprint <https://arxiv.org/abs/1605.07146>*, 2017.
- Hongyang Zhang, Yaodong Yu, Jiantao Jiao, Eric Xing, Laurent El Ghaoui, and Michael Jordan. Theoretically principled trade-off between robustness and accuracy. In *Proceedings of the 36th International Conference on Machine Learning (ICML)*, volume 97, pages 7472–7482, 2019.

## 7 Checklist

1. For all authors...
  - (a) Do the main claims made in the abstract and introduction accurately reflect the paper's contributions and scope? [Yes]
  - (b) Did you describe the limitations of your work? [Yes] The theoretical results are limited by their assumptions in section 4.
  - (c) Did you discuss any potential negative societal impacts of your work? [Yes] Below the conclusion.
  - (d) Have you read the ethics review guidelines and ensured that your paper conforms to them? [Yes]
2. If you are including theoretical results...
  - (a) Did you state the full set of assumptions of all theoretical results? [Yes] In section 4.
  - (b) Did you include complete proofs of all theoretical results? [Yes] Proofs are given in supplement A.
3. If you ran experiments...
  - (a) Did you include the code, data, and instructions needed to reproduce the main experimental results (either in the supplemental material or as a URL)? [Yes] We extended the description of datasets, models and training procedure from section 5 in supplement B and provided the code used in the main paper in the supplemental material.
  - (b) Did you specify all the training details (e.g., data splits, hyperparameters, how they were chosen)? [Yes] Details for the experiments which are not mention in section 5 are given in supplement B.
  - (c) Did you report error bars (e.g., with respect to the random seed after running experiments multiple times)? [Yes] Partially, where it was applicable and interesting (c.f. table 2).
  - (d) Did you include the total amount of compute and the type of resources used (e.g., type of GPUs, internal cluster, or cloud provider)? [Yes] All experiments are run on one NVIDIA GeForce RTX 2080 Ti and package version requirements for the virtual environment are given in the code base.
4. If you are using existing assets (e.g., code, data, models) or curating/releasing new assets...
  - (a) If your work uses existing assets, did you cite the creators? [Yes] Main python packages and models are cited in the paper as well as highlighted in the code.
  - (b) Did you mention the license of the assets? [Yes] The used code bases from others were published under MIT license.
  - (c) Did you include any new assets either in the supplemental material or as a URL? [N/A] Not applicable.
  - (d) Did you discuss whether and how consent was obtained from people whose data you're using/curating? [N/A] Not applicable.
  - (e) Did you discuss whether the data you are using/curating contains personally identifiable information or offensive content? [N/A] Not applicable.
5. If you used crowdsourcing or conducted research with human subjects...
  - (a) Did you include the full text of instructions given to participants and screenshots, if applicable? [N/A] Not applicable.
  - (b) Did you describe any potential participant risks, with links to Institutional Review Board (IRB) approvals, if applicable? [N/A] Not applicable.
  - (c) Did you include the estimated hourly wage paid to participants and the total amount spent on participant compensation? [N/A] Not applicable.

## Supplement

### A Proofs

In this section we proof the theorems of the main paper and recap the needed definitions to do so.

**Definition A.1** (Maximum magnitude attack). Given a multi-class classifier  $f(\cdot)$ , a loss function  $\mathcal{L}(\cdot, \cdot)$ ,  $\ell_p$ -norm  $\|\cdot\|_p$  and a given perturbation strength  $\eta$  the optimization problem for a maximum magnitude attack can be written as

$$\text{maximize } \mathcal{L}(f(x + \delta), y), \text{ w.r.t. } \delta \text{ s.t. } \|\delta\|_p \leq \eta. \quad (5)$$

**Theorem A.1** (Sufficient and necessary robustness condition for linear classifiers). Let  $f : \mathbb{R}^d \times \Omega^h \rightarrow \mathbb{R}^k$  be a stochastic classifier with linear discriminant functions and  $f^A$  and  $f^I$  be two MC estimates of the classifier. Let  $x \in \mathbb{R}^d$  be a data point with label  $y \in \{1, \dots, k\}$  and  $\arg \max_c f_c^A(x) = \arg \max_c f_c^I(x) = y$ , and let  $x_{adv} = x + \delta^A$  be an adversarial example computed for solving the minimization problem (5) for  $f^A$ . It holds that  $\arg \max_c f_c^I(x + \delta^A) = y$  if and only if

$$\min_{c \neq y} \tilde{r}_c^I > \|\delta^A\|_2, \text{ with} \quad (6)$$

$$\tilde{r}_c^I = \begin{cases} \infty, & \text{if } \cos(\alpha_c^{I,A}) = \frac{\langle -\nabla_x(f_y^I(x) - f_c^I(x)), \delta^A \rangle}{\|\nabla_x(f_y^I(x) - f_c^I(x))\|_2 \cdot \|\delta^A\|_2} \leq 0 \\ \frac{f_y^I(x) - f_c^I(x)}{\|\nabla_x(f_y^I(x) - f_c^I(x))\|_2 \cdot \cos(\alpha_c^{I,A})}, & \text{otherwise,} \end{cases}$$

where  $\alpha_c^{I,A}$  is the angle between  $-\nabla_x(f_y^I(x) - f_c^I(x))$  and  $\delta^A$ .

*Proof.* An adversarial attack on  $f^I$  with the adversarial example  $x + \delta^A$  is not successful iff  $\forall c \in \{1, 2, \dots, k\}, c \neq y$ :

$$f_y^I(x + \delta^A) - f_c^I(x + \delta^A) > 0.$$

With Taylor expansion around  $x$  we can rewrite  $f_y^I(x + \delta^A) - f_c^I(x + \delta^A)$  as

$$\begin{aligned} & f_y^I(x) + \langle \nabla_x f_y^I(x), \delta^A \rangle - f_c^I(x) - \langle \nabla_x f_c^I(x), \delta^A \rangle \\ &= f_y^I(x) - f_c^I(x) + \langle \nabla_x f_y^I(x) - \nabla_x f_c^I(x), \delta^A \rangle \\ &= f_y^I(x) - f_c^I(x) - \|\nabla_x(f_y^I(x) - f_c^I(x))\|_2 \cdot \|\delta^A\|_2 \cdot \cos(\alpha_c^{I,A}) \end{aligned} \quad (7)$$

where  $\alpha_c^{I,A} := \angle(-\nabla_x(f_y^I(x) - f_c^I(x)), \delta^A)$ . We can distinguish two cases for each  $c$ .

**Case 1:**  $\cos(\alpha_c^{I,A}) \leq 0$ . In this case last term of eq. (7) is negative or zero and thus

$$f_y^I(x + \delta^A) - f_c^I(x + \delta^A) \geq f_y^I(x) - f_c^I(x) > 0,$$

where the second inequality holds since  $\arg \max_c f_c^I(x) = y$ .

**Case 2:**  $\cos(\alpha_c^{I,A}) > 0$ . In this case the last term of equation eq. (7) is positive and thus

$$f_y^I(x + \delta^A) - f_c^I(x + \delta^A) \leq f_y^I(x) - f_c^I(x).$$

As we see from rearranging eq. (7), it holds  $f_y^I(x + \delta^A) - f_c^I(x + \delta^A) > 0$  if

$$\tilde{r}_c^I := \frac{f_y^I(x) - f_c^I(x)}{\|\nabla_x(f_y^I(x) - f_c^I(x))\|_2 \cdot \cos(\alpha_c^{I,A})} > \|\delta^A\|_2. \quad (8)$$

For each class  $c$  either case 1 holds and we define  $\tilde{r}_c^I := \infty$ , or condition (8) is fulfilled, which yields the condition stated in the theorem.  $\square$

In the main part of the paper we relaxed the linear classifier assumption by  $L$ -smoothness, which was defined as follows:

**Definition A.2** (*L-smoothness* [Yang et al., 2022]). A differentiable function  $f : \mathbb{R}^d \rightarrow \mathbb{R}^k$  is *L-smooth*, if for any  $x_1, x_2 \in \mathbb{R}^d$  and any output dimension  $c \in \{1, \dots, k\}$ :

$$\frac{\|\nabla_{x_1} f_c(x_1) - \nabla_{x_2} f_c(x_2)\|_2}{\|x_1 - x_2\|_2} \leq L .$$

Next we restate one property of *L-smooth* functions which we will use in our proof of theorem 2.

**Proposition A.2** (Bubeck [2015]). *Let  $f$  be an  $L$ -smooth function on  $\mathbb{R}^n$ . For any  $x, y \in \mathbb{R}^n$  it holds:*

$$|f(y) - f(x) - \langle \nabla_x f(x), y - x \rangle| \leq \frac{L}{2} \|y - x\|_2^2 .$$

*Proof.* From the fundamental theorem of calculus we know that for a differentiable function  $f$  it holds that  $f(y) - f(x) = \int_x^y \nabla_t f(t) dt$ . By substituting  $x_t = x + t(y - x)$  we see that  $x_0 = x$  and  $x_1 = y$  and thus we can write  $f(y) - f(x) = \int_0^1 \nabla f(x + t(y - x))^T \cdot (y - x) dt$ . This allows the following approximations

$$\begin{aligned} & |f(y) - f(x) - \langle \nabla_x f(x), y - x \rangle| \\ &= \left| \int_0^1 \nabla f(x + t(y - x))^T \cdot (y - x) dt - (\nabla_x f(x))^T (y - x) \right| \\ &\leq \int_0^1 |(\nabla f(x + t(y - x)) - \nabla_x f(x))^T \cdot (y - x)| dt \\ &\stackrel{\text{Cauchy-Schwarz}}{\leq} \int_0^1 \|\nabla f(x + t(y - x)) - \nabla_x f(x)\|_2 \cdot \|y - x\|_2 dt \\ &\stackrel{L\text{-smoothness}}{\leq} L \cdot \|y - x\|_2^2 \cdot \int_0^1 t dt \\ &= \frac{L}{2} \cdot \|y - x\|_2^2 . \end{aligned}$$

□

**Theorem A.3** (Sufficient condition for the robustness of an *L-smooth* stochastic classifier). *Let  $f : \mathbb{R}^d \times \Omega^h \rightarrow \mathbb{R}^k$  be a stochastic classifier with  $L$ -smooth discriminant functions and  $f^A$  and  $f^I$  be two MC estimates of the prediction. Let  $x \in \mathbb{R}^d$  be a data point with label  $y \in \{1, \dots, k\}$  and  $\arg \max_c f_c^A(x) = \arg \max_c f_c^I(x) = y$ , and let  $x_{adv} = x + \delta^A$  be an adversarial example computed for solving the minimization problem (5) for  $f^A$ . It holds that  $\arg \max_c f_c^I(x + \delta^A) = y$  if*

$$\min_{c \neq y} r_c^I > \|\delta^A\|_2 ,$$

with

$$r_c^I = \begin{cases} \infty , & \text{if } \|\nabla_x (f_y^I(x) - f_c^I(x))\|_2 \cdot \cos(\alpha_c^{I,A}) + \frac{L}{2} \cdot \|\delta^A\|_2 \leq 0, \\ \frac{f_y^I(x) - f_c^I(x)}{\|\nabla_x (f_y^I(x) - f_c^I(x))\|_2 \cdot \cos(\alpha_c^{I,A}) + \frac{L}{2} \cdot \|\delta^A\|_2} , & \text{else} \end{cases}$$

and

$$\cos(\alpha_c^{I,A}) = \frac{\langle -\nabla_x (f_y^I(x) - f_c^I(x)), \delta^A \rangle}{\|\nabla_x (f_y^I(x) - f_c^I(x))\|_2 \cdot \|\delta^A\|_2} .$$

*Proof.* For better readability we write  $f_{y-c}^{\mathcal{I}}(x) := f_y^{\mathcal{I}}(x) - f_c^{\mathcal{I}}(x)$ . Using the result from proposition A.2 and reordering the terms, we get the following lower bound:

$$\begin{aligned}
& f_{y-c}^{\mathcal{I}}(x + \delta^{\mathcal{A}}) \\
& \geq f_{y-c}^{\mathcal{I}}(x) + \langle \nabla_x(f_{y-c}^{\mathcal{I}}(x)), \delta^{\mathcal{A}} \rangle - \frac{L}{2} \cdot \|\delta^{\mathcal{A}}\|_2^2 \\
& = f_{y-c}^{\mathcal{I}}(x) - \langle -\nabla_x(f_{y-c}^{\mathcal{I}}(x)), \delta^{\mathcal{A}} \rangle - \frac{L}{2} \cdot \|\delta^{\mathcal{A}}\|_2^2 \\
& = f_{y-c}^{\mathcal{I}}(x) - \|\nabla_x f_{y-c}^{\mathcal{I}}(x)\|_2 \cdot \|\delta^{\mathcal{A}}\|_2 \cdot \cos(\alpha_c^{\mathcal{I}, \mathcal{A}}) - \frac{L}{2} \cdot \|\delta^{\mathcal{A}}\|_2^2 \\
& = f_{y-c}^{\mathcal{I}}(x) - \left( \|\nabla_x f_{y-c}^{\mathcal{I}}(x)\|_2 \cdot \cos(\alpha_c^{\mathcal{I}, \mathcal{A}}) + \frac{L}{2} \cdot \|\delta^{\mathcal{A}}\|_2 \right) \cdot \|\delta^{\mathcal{A}}\|_2 . \tag{9}
\end{aligned}$$

If eq. (9) is bigger than zero, the attack cannot be successful. Hence,

$$f_{y-c}^{\mathcal{I}}(x) - \left( \|\nabla_x f_{y-c}^{\mathcal{I}}(x)\|_2 \cdot \cos(\alpha_c^{\mathcal{I}, \mathcal{A}}) + \frac{L}{2} \cdot \|\delta^{\mathcal{A}}\|_2 \right) \cdot \|\delta^{\mathcal{A}}\|_2 \stackrel{!}{>} 0 \tag{10}$$

$$f_{y-c}^{\mathcal{I}}(x) > \left( \|\nabla_x f_{y-c}^{\mathcal{I}}(x)\|_2 \cdot \cos(\alpha_c^{\mathcal{I}, \mathcal{A}}) + \frac{L}{2} \cdot \|\delta^{\mathcal{A}}\|_2 \right) \cdot \|\delta^{\mathcal{A}}\|_2 . \tag{11}$$

**Case 1:**  $\|\nabla_x f_{y-c}^{\mathcal{I}}(x)\|_2 \cdot \cos(\alpha_c^{\mathcal{I}, \mathcal{A}}) + \frac{L}{2} \cdot \|\delta^{\mathcal{A}}\|_2 > 0$ . Transforming eq. (11) leads to

$$\frac{f_{y-c}^{\mathcal{I}}(x)}{\|\nabla_x f_{y-c}^{\mathcal{I}}(x)\|_2 \cdot \cos(\alpha_c^{\mathcal{I}, \mathcal{A}}) + \frac{L}{2} \cdot \|\delta^{\mathcal{A}}\|_2} > \|\delta^{\mathcal{A}}\|_2 .$$

**Case 2:**  $\|\nabla_x f_{y-c}^{\mathcal{I}}(x)\|_2 \cdot \cos(\alpha_c^{\mathcal{I}, \mathcal{A}}) + \frac{L}{2} \cdot \|\delta^{\mathcal{A}}\|_2 = 0$ . In this case eq. (10) is trivially fulfilled because  $f_{y-c}^{\mathcal{I}}(x) > 0$  per definition.

**Case 3:**  $\|\nabla_x f_{y-c}^{\mathcal{I}}(x)\|_2 \cdot \cos(\alpha_c^{\mathcal{I}, \mathcal{A}}) + \frac{L}{2} \cdot \|\delta^{\mathcal{A}}\|_2 < 0$ . For this case we get, that

$$-\frac{f_{y-c}^{\mathcal{I}}(x)}{\|\nabla_x f_{y-c}^{\mathcal{I}}(x)\|_2 \cdot \cos(\alpha_c^{\mathcal{I}, \mathcal{A}}) + \frac{L}{2} \cdot \|\delta^{\mathcal{A}}\|_2} < \|\delta^{\mathcal{A}}\|_2 ,$$

which is always guaranteed based on the initial assumption that the benign input was classified correctly, which concludes the proof.  $\square$

The following proposition relates to footnote 5 from the main paper. We show, that the interval, in which the expectation of the gradient norm lies, decreases to the true length of  $\mu$  with reducing the covariance.

**Proposition A.4.** *Let  $X$  be an  $n$ -dimensional random vector following a multivariate normal distribution with mean vector  $\mu$  and diagonal covariance matrix  $\Sigma$ . Then the expectation of  $\|X\|_2$  can be upper and lower bounded by*

$$\|\mu\|_2 \leq \mathbb{E}[\|X\|_2] \leq \sqrt{\|\mu\|_2^2 + \text{tr}(\Sigma)} .$$

*Proof.* We first look at the lower bound which by convexity of the norm and Jensen inequality can be derived via

$$\mathbb{E}[\|X\|_2] \leq \|\mathbb{E}[X]\|_2 = \|\mu\|_2 .$$

Let  $X' \sim \mathcal{N}(0, \mathbf{1}_n)$ , with  $\mathbf{1}_n$  an  $n \times n$ -dimensional unit matrix. With Jensen inequality and concavity of the square-root function we derive the upper bound

$$\begin{aligned}
\mathbb{E}[\|X\|_2] & = \mathbb{E} \left[ \|\mu + X' \cdot \Sigma^{1/2}\|_2 \right] \\
& \leq \left( \mathbb{E} \left[ \left\| \mu + X' \cdot \Sigma^{1/2} \right\|_2^2 \right] \right)^{1/2} \\
& = \left( \|\mu\|_2^2 + 2\mu^T \Sigma^{1/2} \mathbb{E}[X'] + \mathbb{E} \left[ X'^T \Sigma^{1/2T} \Sigma^{1/2} X' \right] \right)^{1/2} \\
& = \sqrt{\|\mu\|_2^2 + \text{tr}(\Sigma)} .
\end{aligned}$$

□

## B Additional information on datasets, models and training

In the following we describe additional details on the datasets, models and training procedures which were not stated in the main paper due to space restrictions. Additionally, please find the code for the results in the main paper attached in the supplementary material.

### B.1 Datasets

We used three well know datasets: FashionMNIST [Xiao et al., 2017], CIFAR10 and CIFAR100 [Krizhevsky et al., b], which consist out of 60,000 training and 10,000 test images of dimension  $28 \times 28$  or  $32 \times 32 \times 3$  in case of CIFAR where each image is uniquely associated to one out of 10 or 100 possible labels. We took all datasets from the torchvision package with the predefined training and test split.

### B.2 Models trained on FashionMNIST

For training the BNN and IM we used the exact same hyperparameters. First, we assumed a standard normal prior decomposed as matrix variate normal distributions for the BNN and approximated the posterior distribution via maximizing the evidence lower bound (ELBO). For the IM we added a Kullback-Leibler distance from the trained parameter distribution to a standard matrix variate normal distribution as a regularization term. For both models we used a batch size of 100 and trained for 50 epochs with Adam [Kingma and Ba, 2015] and an initial learning rate of 0.001. To leverage the difference between IM and BNN we used 5 samples to approximate the expectation in the ELBO/IM-objective. We used the same learning rate, batch size, optimizer and amount of epochs for training the stochastic input networks. During a forward pass in training we created and used five noisy versions of each input, where the noise was drawn from a centered Gaussian distribution with variance 0.05 or 0.1 and the average prediction was fed into the cross-entropy loss.

### B.3 Models trained on CIFAR10

As stated in the main part, we used the wide ResNet [Zagoruyko and Komodakis, 2017] of depth 28 and widening factor 10 provided by <https://github.com/meliketoy/wide-resnet.pytorch> with dropout probabilities 0.3 and 0.6 and also used the learning hyperparameters provided with the code which are: training for 200 epochs with batch size 100, stochastic gradient descent as optimizer with momentum 0.9, weight decay  $5e-4$  and a scheduled learning rate decreasing from an initial 0.1 for epoch 0-60 to 0.02 for 60-120 and lastly 0.004 for epochs 120-200.

## C Additional experimental results

In this section we present the results which were not shown in the main part due to space restrictions.

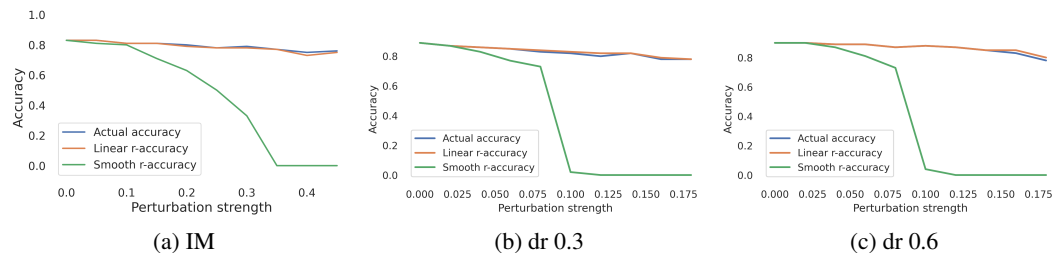


Figure 7: Adversarial accuracy of the a) smoothed IM on FashionMNIST and b),c) smoothed ResNet with dropout probability 0.3 and 0.6 on CIFAR10 vs percentage of images for which  $\min_c r_c^{\mathcal{I}} > \|\delta^{\mathcal{A}}\|_2$  (smooth) and  $\min_c \tilde{r}_c^{\mathcal{I}} > \|\delta^{\mathcal{A}}\|_2$  (linear) for 100 images from the respective test sets. Attacks were conducted on the smoothed classifier with using 10 attack samples.

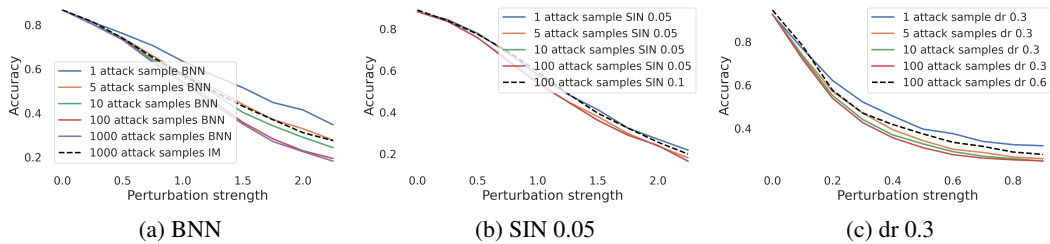


Figure 8: Accuracy under FGM attack for a) the BNN and b) the SIN 0.05 on FashionMNIST and c) ResNet with dropout probability 0.3 on CIFAR10 for different perturbation strengths and amount of samples used for calculating the attack. During inference we used 100 samples.

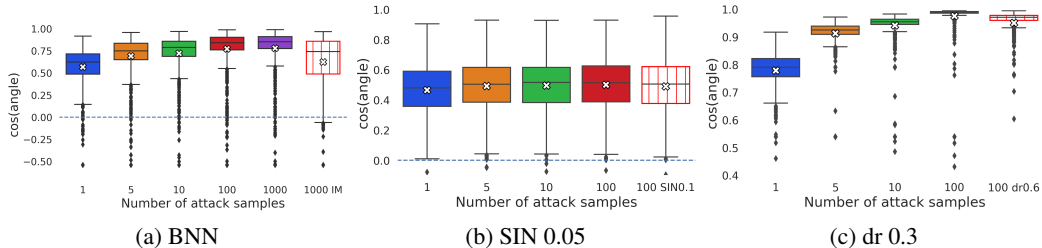


Figure 9: Cosine of the angle for the first 1,000 test set images from the FashionMNIST and CIFAR10 test set for an a) BNN, b) SIN 0.05 and c) ResNet trained with dropout probability 0.3 when attacked with different amounts of samples and attack strength 1.5 and 0.3 with FGM respectively. White crosses indicate the mean value.

## C.1 Complementary experiments on accuracy of robustness conditions

For completeness we attached the results on the transferability of our derived sufficient conditions to: the IM on FashionMNIST and the two ResNet with dropout probability 0.3 and 0.6 on CIFAR10. For the BNN we used the same setting as described in the main paper and derive similar results (c.f. figure 7): while the percentage of samples fulfilling the condition  $\min_c r_c^T > \|\delta^A\|_2$  approaches zero with growing perturbation strength the percentage of samples fulfilling the condition from theorem 1 in the main paper closely matches the real adversarial accuracy in a narrow environment. For models on CIFAR10 we had to adapt the noise added for the smooth classifier to 0.01 and reduce the amount of samples during inference to 50 such that it fits on one GPU.

## C.2 Complementary experiments on stronger attacks

We first present the results not shown in the main paper. That is, we investigate the accuracy under FGM attack with an increasing amount of samples used during the attack (c.f. figure 8). Similar to the observations in the main paper, the accuracy under attack is reduced by an increased amount of samples. However, we observe only a very small decrease in accuracy when increasing the amount of samples from 100 and 1,000 for the BNN, from 1 to 5 or above for the SIN 0.05 and when using 5 instead of 10 or 100 samples for the attack on the ResNet trained with dropout probability 0.3. This observation is mirrored by the reduction of  $\cos(\alpha_c^{T,A})$  displayed in figure 9 where we observe an increase of the cosine boxplots which matches the decrease of the adversarial accuracy when taking more samples during the attack.

### C.2.1 Attacks with FGSM ( $\ell_\infty$ -norm)

All adversarial examples in the main part of the paper were based on an  $\ell_2$ -norm constraint, which we chose for the nice geometric distance interpretation. However, the first proposed attack scheme [Goodfellow et al., 2015] was based on  $\ell_\infty$ -norm, which we test in the following. In figure 10 and 11 we see the respective results on the different data sets. For all models the robustness is decreased with

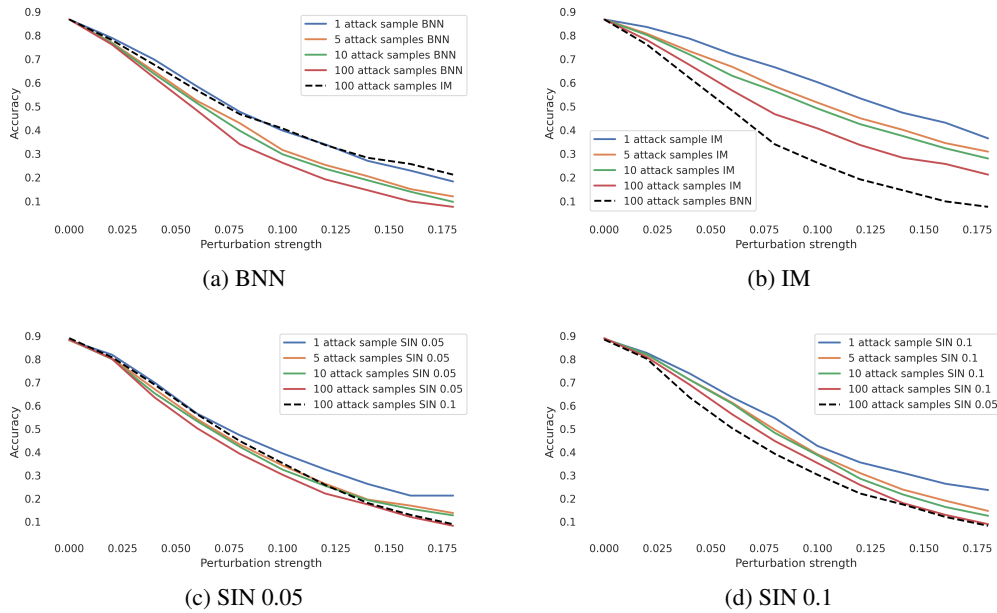


Figure 10: Accuracy under FGSM attack under  $\ell_\infty$ -norm constraint for a) the BNN, b) the IM, c) SIN 0.05 and d) SIN 0.1 on the first 1,000 test set images from FashionMNIST for different perturbation strengths and amount of samples used for calculating the attack. Predictions during inference are based on 100 samples.

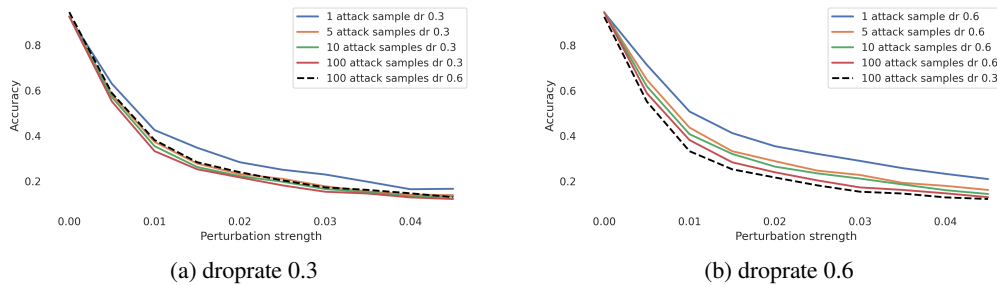


Figure 11: Accuracy under FGSM attack under  $\ell_\infty$ -norm constraint for the ResNet model with a dropout probability a) of 0.3 and b) of 0.6 on the first 1,000 test set images from CIFAR10 for different perturbation strengths and amount of samples used for calculating the attack. Predictions during inference are based on 100 samples.

multiple samples and models with higher prediction variance also have a higher accuracy under this attack. Note, that the values of the perturbation strength are not comparable to the values under  $\ell_2$ -norm constraint, since  $\|x\|_\infty \leq \|x\|_2$ .

### C.2.2 Attacks with PGD

Projected gradient descent [Madry et al., 2018] is a strong iterative attack, where multiple small steps of size  $\nu$  of fast gradient method are applied. Specifically, we used the same  $\ell_2$ -norm length constraint on  $\eta$  as in the experiments of the main part of the paper but chose step size  $\nu = \eta/50$  and 100 iterations. Note that at each iteration a new network is sampled such that for an attack based on 1 samples, 100 different attack networks were seen, for an attack based on 5 samples 500 different networks and so on. In figure 12 and 13 we see that the overall accuracy is decreased compared to the results for FGM, but still, IM has a higher accuracy under attack than the BNN and so does the ResNet with a higher dropout probability. Further, the attacks get stronger with taking more samples, so the general observations made in the main paper also hold for strong attacks and are not due to a sub-optimal attack.

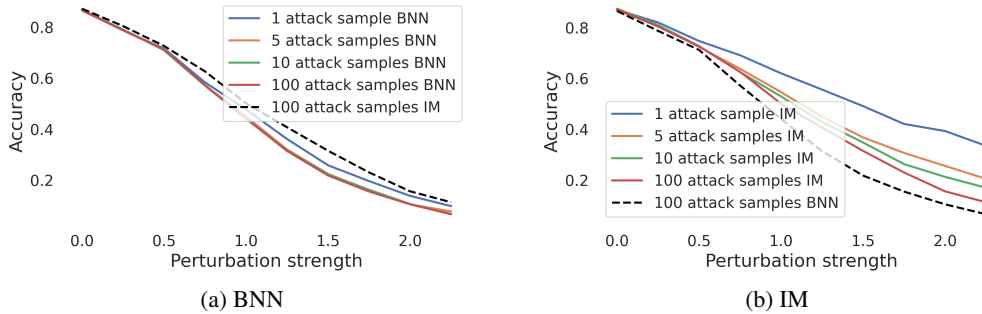


Figure 12: Accuracy under PGD attack with 100 iterations for a) the BNN and b) the IM on the first 1,000 test set images from FashionMNIST for different perturbation strengths and amount of samples used for calculating the attack.

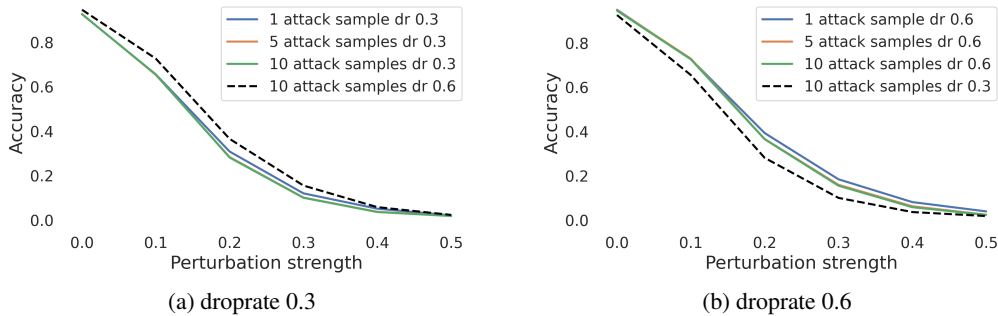


Figure 13: Accuracy under PGD attack with 100 iterations for the ResNet with a dropout probability of a) 0.3 and b) of 0.6 on CIFAR10 for different perturbation strengths and amount of samples used for calculating the attack.

### C.3 Discussing the impact of extreme prediction values

Attacks based on softmax predictions can be unsuccessful for deterministic and stochastic neural networks alike when encountering overly confident predictions. That is, predictions where the softmax output is equal to 1, since these lead to zero gradients. A practical solution to circumvent this problem is to calculate the gradient based on the logits [Carlini and Wagner, 2017a]. This approach is feasible for classifier whose predictions do not depend on the scaling of the output, that is, outputs which are equally expressive in both intervals  $[0, 1]$  and  $[-\infty, \infty]$ . In Bayesian neural networks, where  $f_c(x, \Theta)$  is per definition a probability the shortcut over taking the gradient over logits leads to distorted gradients. For completeness, we nevertheless look at the performance of an attack based on the logits for the two different models trained on FashionMNIST with softmax outputs: IM and BNN. We conducted an adversarial FGM attack based on 100 samples, but instead of using the cross-entropy

loss we used the Carlini-Wagner (CW) loss [Carlini and Wagner, 2017a] on the averaged logits, given by:

$$CW(x, \Theta^A) = \max \left( \max_{i \neq t} (Z(x, \Theta^A)_i) - Z(x, \Theta^A)_t, 0 \right),$$

where  $Z(x, \Theta^A)_t = \frac{1}{S^A} \sum_{s=1}^{S^A} Z(x, \theta_s)_t$  is an arbitrary averaged logit of an output node for input  $x$ . In figure 14 it is shown, that the attack with the CW loss on the infinite mixture model improves upon the original attack scheme (FGM), whereas it did not improve the attack’s success for the BNN. We additionally conducted an attack based on the logit margin loss  $\mathcal{L}(x + \delta^A, y) = -(\min_{c \neq y} f_{y-c}(x))$  equivalent to the attack conducted on the SIN, but we found that it performs similar to the CW loss.

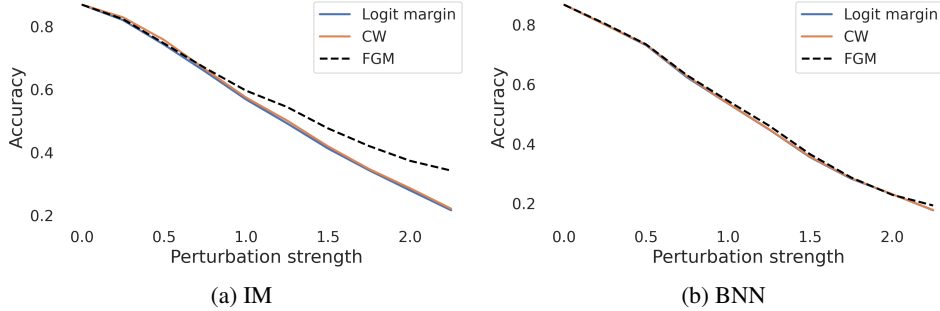


Figure 14: Accuracy under attack for the first 1,000 test set images from FashionMNIST with varying perturbation strengths and different attack objectives. Each attack was calculated based on 100 samples and  $\ell_2$ -constraint for models trained on FashionMNIST.

#### C.4 Complementary experiments on robustness in dependence of the amount of samples used during inference

In the main part of the paper we argued why, surprisingly, the amount of samples during inference does not influence the robustness, even though we see in figure 15 that less sample lead to the smallest values for  $\cos(\alpha_c^{\mathcal{I}, \mathcal{A}})$ . As stated in the main part, the increased gradient norm when using only few samples seems to compensate the assumed benefits with regard to the angle for using few samples (c.f. figure 16). This can also be seen in table 2 and figure 6 from the main paper, where a (negative) effect on the robustness can only be observed for one inference sample, which also leads to the worst test set accuracy. The benign prediction margins are also hardly effected by the increased number of samples during prediction (c.f. figure 17).

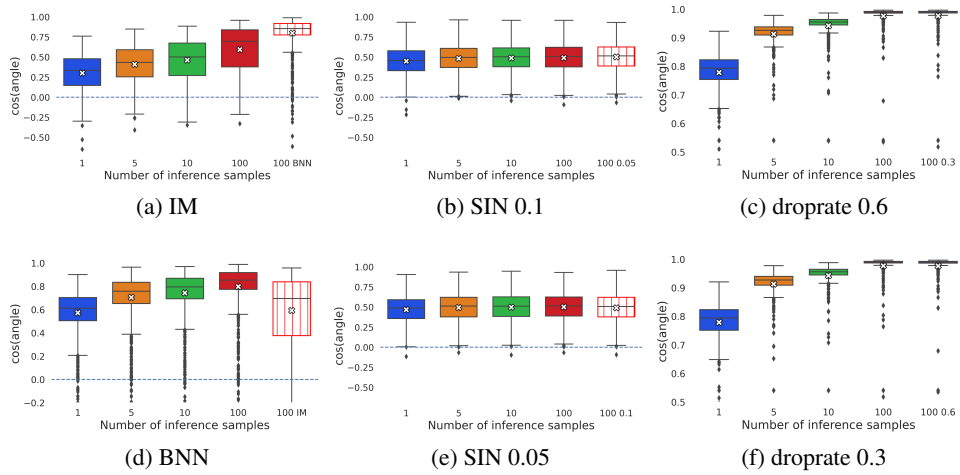


Figure 15: Cosine of the angle for models trained on FashionMNIST ( a ), b), d), e) ) and trained on CIFAR10 ( c ) and f ) for different amounts of samples used during inference. Used attack direction  $\delta$  was calculated based on 100 sample of FGM under  $\ell_2$ -norm constraint with  $\eta = 1.5$  and  $0.3$  respectively.

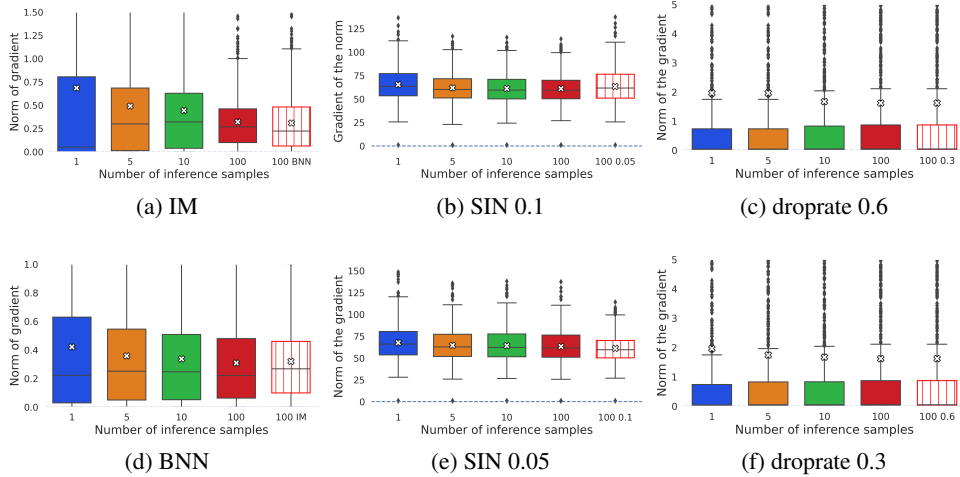


Figure 16: Norm of the gradient for models trained on FashionMNIST ( a ), b), d), e) ) and trained on CIFAR10 ( c ) and f ) for different amounts of samples used during inference.

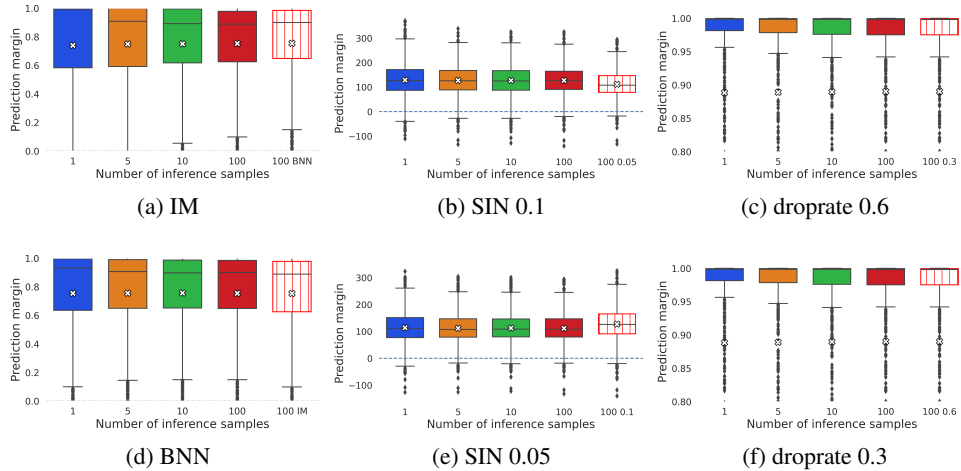


Figure 17: Prediction margin for the benign inputs for models trained on FashionMNIST ( a), b), d), e) and trained on CIFAR10 ( c) and f) ) for different amounts of samples used during inference.

### C.5 Experiments for CIFAR100

For the experiments on CIFAR100 we used yet another method to create stochastic neural networks, namely by applying a Laplace approximation [MacKay, 1992] to an already trained network. This is achieved by adapting a Gaussian distribution over the network’s parameters such that the mean is given by the maximum a posterior estimate and the covariance are calculated to match the local loss curvature. Specifically, we used the GitHub library from Daxberger et al. [2021] on top of the adversarial trained wide ResNet70-16 with clean accuracy 69.15 provided by Gowal et al. [2020]. Because of the high amount of parameters in this network we used a last-layer diagonal Gaussian approximation for fitting our posterior distribution from which we sample the  $\theta_i$ ’s for deriving an approximate expected prediction. As in the previous experiments we observe, that the adversarial accuracy decreases with more samples during attack, while the angle between the attack and negative gradient during inference decreases which leads to a cosine increase.

Table 3: Adversarial accuracy decrease and  $\cos(\alpha_c^{\mathcal{I},\mathcal{A}})$  increase on CIFAR100 with increased amount of samples during attack, where the attack was conducted with  $\ell_\infty$  norm constraint and perturbation strength  $8/225$ .

# SAMPLES	ADVERSARIAL ACCURACY	AVERAGE $\cos(\alpha_c^{\mathcal{I},\mathcal{A}}) \pm \text{STD}$
1	48.00	$0.2028 \pm 0.112$
5	45.00	$0.2550 \pm 0.100$
10	43.90	$0.2680 \pm 0.095$